Full-state Modeling, Motion Planning and Control Of Mobile Manipulators

Costas S. Tzafestas

Institute of Informatics and Telecommunications

National Center for Scientific Research "Demokritos",

Aghia Paraskevi, Attiki,

Athens 15310

GREECE

E-mail: ktzaf@iit.demokritos.gr

Spyros G. Tzafestas

Intelligent Robotics and Automation Laboratory

Department of Electrical and Computer Engineering

National Technical University of Athens

Zographou 15773, Athens

GREECE

E-mail: tzafesta@softlab.ntua.gr

Abstract: This paper provides a full-state dynamic analysis and control design study of mobile manipulator (MM) systems. Specifically, the following problems are addressed: (i) full-state dynamic modeling (including kinematics), (ii) multiple-task motion planning, and (iii) full-state tracking control (feedback linearizing control, sliding mode control). A set of representative results are presented for MMs with nonholonomic and holonomic omnidirectional platforms and 2-DOF or 3-DOF manipulator arms. These and other results verify the expectation that the use of full-state models (i.e. the inclusion in the controller design of the dynamic interaction between the mobile platform and robotic manipulator mounted on it) leads to a much superior tracking capability compared to the situation where the models used are not full-state ones (i.e. some or all of the platform-manipulator interaction terms are neglected).

Keywords: mobile manipulators, full-state modeling, motion planning, full-state control, feedback-linearizing decoupling control, sliding-mode control

Costas S. Tzafestas holds a Diploma in Electrical and Computer Engineering from the National Technical University of Athens, Greece, and a DEA and Ph.D degrees on Robotics from the Université Pierre et Marie Curie (Paris 6), France. He is currently a research associate within the Institute of Informatics and Telecommunications at the National Center for Scientific Research "Demokritos", Athens. His research interests include virtual reality interfaces, haptic feedback, human/machine interaction and telerobotics. He has also worked on robust, adaptive and neural control with applications in walking robots and cooperating manipulators. He is a member of the IEEE and of the Greek Technical Chamber.

Spyros G. Tzafestas is full Professor, Director of the Institute of Communications and Computer Systems (ICCS), the Signals, Control and Robotics Division and the Intelligent Robotics and Automation Laboratory (IRAL) of the National Technical University of Athens (NTUA). Holder of Ph.D. and D.Sc. in Control and Automation. Recipient of Honorary Doctorates of the International University (D.Sc.(Hon.)) and of the Technical University of Munich (Dr.-Ing.E.h.). Fellow of IEEE (N.Y.) and IEE (London); Member of ASME (N.Y.), New York Academy of Sciences, IMACS (Rutgers, N.J.) and SIRES (Brussels). Member of IFAC SECOM and MIM TCs. Project evaluator of national and international projects (USA, Canada, Italy, Hong-Kong, Japan). Project coordinator of national and EU projects in the fields of robotics, CIM and IT (ESPRIT, BRITE-EURAM, TIDE, INTAS, SOCRATES, EUREKA, GROWTH etc.). Publications: 30 research books, 60 book chapters, over 700 journal and conference technical papers. Editor-in-Chief of the Journal of Intelligent and Robotics Systems and of the book series "Microprocessor-Based and Intelligent Systems Engineering" (Kluwer). Organizer of several international conferences (IEEE, IFAC, IMACS, IASTED, SIRES etc.). Current research interests include: control, robotics and CIM.

1. Introduction

Mobile manipulators (MMs), i.e. manipulator arms mounted on mobile platforms, have received increasing attention over the last fifteen years, for both their challenging analytical problems and their large repertory of applications [1-17]. Due to the platform mobility, the system manipulator's workspace is enlarged compared to the fixed manipulator arm, and the robot tasks can be performed in inaccessible or hostile environments for the human operator. However, the motion planning and control problems of a mobile manipulator cannot be faced by traditional methods due to the nonholonomic nature of the system which is imposed by the platform's wheels. Actually, the nonholonomic (nonintegrable) constraints affect the workspace and the trajectory planning of the MM and reduce the flexibility of the available degrees-of- freedom. On the other hand, the MM possesses a complex and strongly coupled dynamic model of the nonholonomic dynamics of the mobile platform and the dynamics of the manipulator arm.

The problem of designing suitable wheel systems for mobile platforms has been considered in [1-7]. Mobile robots with a two-independent driving wheel mechanism or front-wheel or rear-wheel driving

mechanism are now widely used in factory or hospitals but cannot realize a side motion due to the nonholonomic constraint involved. To overcome this difficulty, several holonomic and omnidirectional wheeled platforms have been proposed [3-7].

The multi-task planning problem of MMs has been considered in [8-11]. When an MM performs a multiple task (i.e. a sequence of tasks) the final configuration of each task becomes the initial configuration of the following task. This was named commutation configuration in [8, 9] where the motion planning problem was divided into two subproblems, namely predicting the optimal commutation configuration for each pair of adjacent tasks, and determining the motion trajectory associated with the initial and final configurations for each task via the solution of the corresponding two-point boundary value problem.

Regarding the control of MMs, in most previous studies the control problems were constrained only to partial states of the MM system. But, in many practical situations the tracking control of the full state is a prerequisite for successful operation of the MM. Some studies, where the dynamic interaction between the mobile platform and the robotic manipulator is addressed, have been reported in [12-17]. In particular, the controller derived in [14] was of the decentralized type treating the platform and the manipulator as two separate systems and showing that the two subsystems are stable provided that the unknown interconnections are bounded. In [15] the platform was assumed to have a soft suspension, and a controller was derived which achieves good trajectory tracking despite the softly-suspended platform.

The purpose of this paper is to provide a unified study of MMs with reference to the dynamic interaction of the platform and the manipulator arm. The full-state dynamic model is first provided for both nonholonomic and holonomic/omnidirectional platforms. Then the multiple task motion planning problem is considered along the lines of [11] where there is no need to solve a two-point boundary-value problem. Finally the full-state control problem is treated by three different methods, namely standard computed torque control, feedback linearizing-decoupling control, and sliding-mode robust control [4-6, 16-20]. The paper includes a sufficient set of experimental results for both the motion planning problem and the trajectory tracking control problem via the sliding-mode and the feedback linearizing-decoupling techniques.

2. Full-state Dynamic Modeling of Mobile Manipulators

2.1 Kinematics

Before presenting the full-state dynamic model of MMs we briefly discuss their kinematic model. Consider the MM of Figure 1a where the four principal coordinate frames are shown: world frame O_w, platform frame O_p, manipulator base frame O_b and end effector frame O_e. Then, the manipulator's end effector position/orientation with respect to O_w is given by:

$$ {}^{w}\mathbf{T}_e = {}^{w}\mathbf{T}_p \cdot {}^{p}\mathbf{T}_b \cdot {}^{b}\mathbf{T}_e \tag{1} $$

where ${}^{w}\mathbf{T}_p$ is determined by $\mathbf{p} = [x, y, \varphi]^T$, ${}^{p}\mathbf{T}_b$ is a fixed matrix, and ${}^{b}\mathbf{T}_e$ is determined by the joint variables' vector $\boldsymbol{\theta} = [\theta_1, \theta_2, \ldots, \theta_{n_m}]^T$ where n_m denotes the DOF of the robotic manipulator.

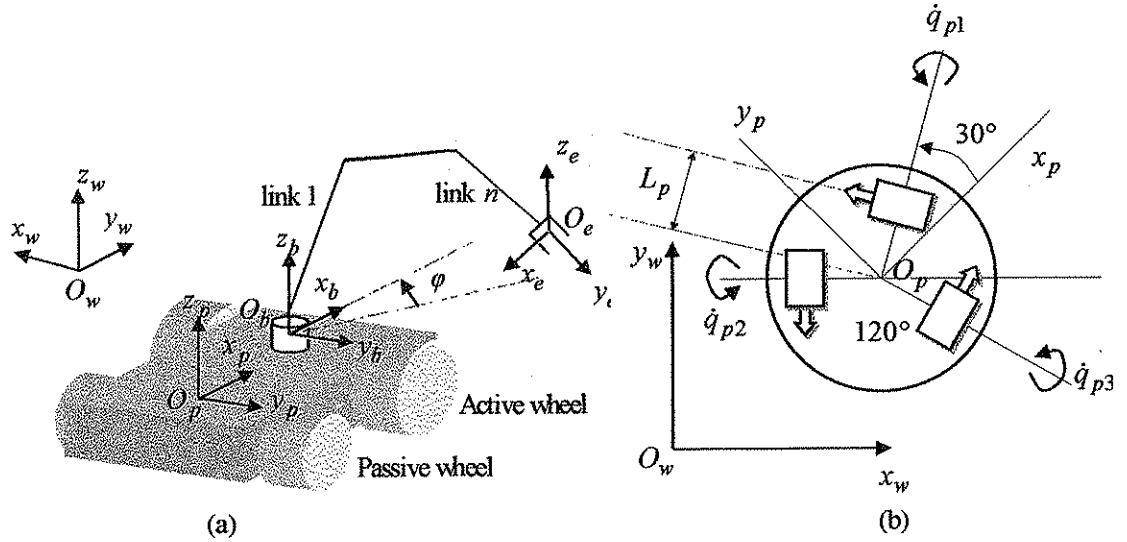

Figure 1. (a) Geometric Features of MM with Conventional Wheels, (b) Geometric Features of Omnidirectional Platform (Three Orthogonal Lateral Wheels)

The end effector's position/orientation vector ${}^{w}\mathbf{x}_e$ is a nonlinear function $\mathbf{f}(\cdot)$ of the MM's overall configuration (posture) vector $\mathbf{q} = [\mathbf{p}^T, \boldsymbol{\theta}^T]^T \in \Re^n$ $(n = 3 + n_m)$, i.e.

$$ {}^{w}\mathbf{x}_e = \mathbf{f}(\mathbf{q}) \tag{2} $$

If $\mathbf{x}_e^d$ is the end effector's desired $m-D$ task vector, then one must have

$$ {}^{w}\mathbf{x}_e = \mathbf{x}_e^d = \mathbf{f}(\mathbf{q}) \tag{3} $$

which upon differentiation gives

$$ \dot{\mathbf{x}}_e^d = \mathbf{J}(\mathbf{q}) \cdot \dot{\mathbf{q}} \tag{4} $$

where $\mathbf{J}(\mathbf{q})$ is the $m \times n$ Jacobian matrix of the MM. If the platform is nonholonomic without wheel-floor slipping, then the following constraint holds:

$$ \mathbf{G}(\mathbf{q}) \cdot \dot{\mathbf{q}} = 0, \ \mathbf{G}(\mathbf{q}) = [\sin\varphi, -\cos\varphi, 0, \ldots, 0] \tag{5} $$

where $\dot{\mathbf{q}}$ cannot be eliminated by integration to give $\mathbf{G}'(\mathbf{q}) = 0$. Thus, Eqs (4) and (5) can be combined to give

$$ \dot{\mathbf{x}} = \mathbf{J}_e(\mathbf{q}) \cdot \dot{\mathbf{q}}, \ \mathbf{x} = \begin{bmatrix} \mathbf{x}_e^d \\ \hline 0 \end{bmatrix}, \ \mathbf{J}_e(\mathbf{q}) = \begin{bmatrix} \mathbf{J}(\mathbf{q}) \\ \hline \mathbf{G}(\mathbf{q}) \end{bmatrix} \tag{6} $$

Clearly, the actual form of $\mathbf{J}_e(\mathbf{q})$ depends on the particular type of the wheels, the platform and the manipulator. For an omnidirectional MM with lateral/orthogonal wheels, the form of $\mathbf{J}_e(\mathbf{q})$ is provided in [4-6].

2.2 Dynamics

The MMs dynamics is governed by the Euler-Lagrange equations subject to the constraint:

$$\frac{d}{dt}\frac{\partial L}{\partial \dot{\boldsymbol{q}}}-\frac{\partial L}{\partial \boldsymbol{q}}+\mathbf{G}^T(\boldsymbol{q})\boldsymbol{\lambda}=\tau \tag{7}$$

where L is the Lagrangian of the MM, and $\boldsymbol{\lambda}$ the Lagrange multiplier vector. Introducing in (7) the expression for $L=K-P$ (K=kinetic energy and P=potential energy) it is not difficult to derive the following dynamic models (see e.g. [14, 16, 17]).

Platform Dynamics

$$\begin{aligned}&\mathbf{M}_{p_1}(\mathbf{q}_p)\ddot{\mathbf{q}}_p+\mathbf{C}_{p_1}(\mathbf{q}_p,\dot{\mathbf{q}}_p)+\mathbf{C}_{p_2}(\mathbf{q}_p,\mathbf{q}_m;\dot{\mathbf{q}}_p,\dot{\mathbf{q}}_m)\\&=\mathbf{E}_p\tau_p-\mathbf{G}^T(\mathbf{q}_p)\boldsymbol{\lambda}-\mathbf{M}_{p_2}(\mathbf{q}_p,\mathbf{q}_m)\ddot{\mathbf{q}}_p-\mathbf{D}(\mathbf{q}_p,\mathbf{q}_m)\ddot{\mathbf{q}}_m\end{aligned} \tag{8a}$$

Manipulator Dynamics

$$\begin{aligned}&\mathbf{M}_m(\mathbf{q}_m)\ddot{\mathbf{q}}_m+\mathbf{C}_{m_1}(\mathbf{q}_m,\dot{\mathbf{q}}_m)+\mathbf{C}_{m_2}(\mathbf{q}_m,\dot{\mathbf{q}}_m;\dot{\mathbf{q}}_p)\\&=\tau_m-\mathbf{D}_m(\mathbf{q}_p,\mathbf{q}_m)\ddot{\mathbf{q}}_p\end{aligned} \tag{8b}$$

where $\mathbf{E}_p$ is an 4×2 constant matrix, $\mathbf{q}_m$ is manipulator's joint variables' vector, and $\mathbf{q}_p=[x_p,y_p,\theta_r,\theta_l]^T$ (see Figure 1). Combining the inertia and velocity terms, Eqs (8a) and (8b) are simplified as:

$$\begin{aligned}&\mathbf{M}_p(\mathbf{q}_p,\mathbf{q}_m)\ddot{\mathbf{q}}_p+\mathbf{C}_p(\mathbf{q}_p,\mathbf{q}_m;\dot{\mathbf{q}}_p,\dot{\mathbf{q}}_m)\\&=\mathbf{E}_p\tau_p-\mathbf{G}^T\boldsymbol{\lambda}-\mathbf{D}_p(\mathbf{q}_p,\mathbf{q}_m)\ddot{\mathbf{q}}_m\end{aligned} \tag{9a}$$

$$\begin{aligned}&\mathbf{M}_m(\mathbf{q}_m)\ddot{\mathbf{q}}_m+\mathbf{C}_m(\mathbf{q}_p,\mathbf{q}_m;\dot{\mathbf{q}}_p)\\&=\tau_m-\mathbf{D}_m(\mathbf{q}_p,\mathbf{q}_m)\ddot{\mathbf{q}}_p\end{aligned} \tag{9b}$$

To write the full-state dynamic model (9a,b) in state-space form we first write the platform velocity $\dot{\mathbf{q}}_p$ as:

$$\dot{\mathbf{q}}_p=\mathbf{F}(\mathbf{q}_p)\mathbf{v}(t) \tag{10}$$

where $\mathbf{v}(t)$ is a suitable vector of generalized velocities and $\mathbf{F}(\mathbf{q}_p)$ is a full rank 4×2 matrix whose columns are in the null space of $\mathbf{G}(\mathbf{q}_p)$ (due to the constraint $\mathbf{G}(\dot{\mathbf{q}}_p)\cdot\dot{\mathbf{q}}_p=0$).

Then we premultiply Eq (9a) by $\mathbf{F}^T$ and carry out the calculations taking into account Eq (10) and the fact that $\mathbf{F}^T\mathbf{G}^T=0$ to obtain:

$$\mathbf{F}^T\left(\mathbf{M}_p\mathbf{F}\dot{\mathbf{v}}+\mathbf{M}_p\dot{\mathbf{F}}\mathbf{v}+\mathbf{C}_p\right)=\mathbf{F}^T\mathbf{E}_p\mathbf{r}_p-\mathbf{F}^T\mathbf{D}_p\ddot{\mathbf{q}}_m \tag{11a}$$

Similarly, Eq (9b) gives:

$$\mathbf{M}_m\ddot{\mathbf{q}}_m+\mathbf{C}_m=\mathbf{r}_m-\mathbf{D}_m\dot{\mathbf{F}}\mathbf{v}-\mathbf{D}_m\mathbf{F}\dot{\mathbf{v}} \tag{11b}$$

Finally, Eq (11a, b) can be written in the desired full state space form:

$$\dot{\mathbf{x}}=\mathbf{a}(\mathbf{x})+\mathbf{B}(x)\tau\ ,\ \tau=[\tau_p^T,\tau_m^T]^T \tag{12}$$

$$\mathbf{x}=\begin{bmatrix}\mathbf{x}_1\\ \mathbf{x}_2\\ \mathbf{x}_3\end{bmatrix}=\begin{bmatrix}\mathbf{q}_p\\ \mathbf{q}_m\\ \mathbf{v}\\ \dot{\mathbf{q}}_m\end{bmatrix},\ \mathbf{a}(x)=\begin{bmatrix}\mathbf{F}\mathbf{v}\\ \dot{\mathbf{q}}_m\\ \mathbf{K}^{-1}\mathbf{C}\end{bmatrix},\ \mathbf{B}(x)=\begin{bmatrix}\mathbf{0}\\ \mathbf{0}\\ \mathbf{K}^{-1}\mathbf{S}\end{bmatrix} \tag{13a}$$

$$\mathbf{K}=\begin{bmatrix}\mathbf{F}^T\mathbf{M}_p\mathbf{F} & \mathbf{F}^T\mathbf{D}_p\\ \mathbf{D}_m\mathbf{F} & \mathbf{M}_m\end{bmatrix},\ \mathbf{S}=\begin{bmatrix}\mathbf{F}^T\mathbf{E}_p & 0\\ 0 & \mathbf{I}\end{bmatrix},\ \mathbf{C}=\begin{bmatrix}-\mathbf{F}^T\mathbf{M}_p\dot{\mathbf{F}}\mathbf{v}-\mathbf{F}^T\mathbf{C}_p\\ -\mathbf{C}_m-\mathbf{D}_m\dot{\mathbf{F}}\mathbf{v}\end{bmatrix} \tag{13b}$$

Here

$$\mathbf{G}(\mathbf{q}_p)=\begin{bmatrix}-\sin\varphi & \cos\varphi & 0 & 0\\ -\cos\varphi & -\sin\varphi & r/2 & r/2\end{bmatrix} \tag{14}$$

and so a possible selection for $\mathbf{F}(\mathbf{q}_p)$ is

$$\mathbf{F}(\mathbf{q}_p)=\begin{bmatrix}\cos\varphi & \cos\varphi\\ \sin\varphi & \sin\varphi\\ 2/r & 0\\ 0 & 2/r\end{bmatrix} \tag{15}$$

With $\mathbf{F}(\mathbf{q}_p)$ as in (15) one can have $\mathbf{F}^T\mathbf{E}_p=\frac{2}{r}\mathbf{I}$ in which case $\mathbf{S}$ is invertible. For the case of the omnidirectional MM mentioned in Section 2.1 the above full state model (12) was derived in [4-6]. The model for an 1-DOF manipulator mounted on a mobile platform with a 2-DOF suspension system is derived in [21].

3. Full-state Motion Planning of Mobile Manipulators

A single task for the MM's end effector is to follow a desired trajectory in the world coordinate frame. The platform is assumed to have a nonholonomic constraint of the type (5). The MM must perform a multiple task consisting of N consecutive single tasks. In doing this a certain objective criterion should be optimized, e.g. obstacle avoidance, singular configuration avoidance, best utilization of actuator torque, etc. If the criterion to be optimized for each task is $V_i(\mathbf{q}_i,\dot{\mathbf{q}}_i)$, $i=1,2,...,N$, where $\mathbf{q}=[\mathbf{p}^T,\boldsymbol{\theta}^T]^T$, the multiple-task motion planning problem is formulated as follows:

Find the motion trajectory $\{\mathbf{q}_1(t),\mathbf{q}_2(t),...,\mathbf{q}_n(t)\}$, which minimizes the total cost function:

$$V_o(\mathbf{q}_1,\mathbf{q}_2,...,\mathbf{q}_N;\dot{\mathbf{q}}_1,\dot{\mathbf{q}}_2,...,\dot{\mathbf{q}}_N)=\sum_{i=1}^{N}\mu_i\int_{t_{io}}^{t_{if}}V_i\big(\mathbf{q}_i(t),\dot{\mathbf{q}}_i(t)\big)dt \tag{16}$$

subject to the equality kinematic constraints:

$$\mathbf{x}_{e,i}^d=\mathbf{f}_i(\mathbf{q}_i)\ \text{and}\ \mathbf{G}_i(\mathbf{q}_i)\cdot\dot{\mathbf{q}}_i=0,\ i=1,2,...,N \tag{17}$$

where i represents the i-th task, μ_i is a weighting constant associated with the i-th objective function, and t_{io}, t_{if} are the initial and final times of the i-th task.

The constrained optimization problem {(16),(17)} can be converted to an unconstrained optimization

problem if V_i in (16) is replaced by the Lagrangian function:

$$L_i(\mathbf{q}_i,\dot{\mathbf{q}}_i;\boldsymbol{\lambda}_{ei},\boldsymbol{\lambda}_{gi}) = V_i(\mathbf{q}_i,\dot{\mathbf{q}}_i) + \boldsymbol{\lambda}_{ei}\left[\mathbf{x}_{e,i}^d - \mathbf{f}_i(\mathbf{q}_i)\right] + \boldsymbol{\lambda}_{g,i}\mathbf{G}_i(\mathbf{q}_i)\cdot\dot{\mathbf{q}}_i \tag{18}$$

The necessary conditions for optimality are found to be:

$$\frac{\partial L_i}{\partial \mathbf{q}_i} - \frac{d}{dt}\left(\frac{\partial L_i}{\partial \dot{\mathbf{q}}_i}\right) = 0 \tag{19a}$$

$$\frac{\partial L_i}{\partial \boldsymbol{\lambda}_{e,i}} = 0, \text{ i.e. } \mathbf{x}_{e,i}^d - \mathbf{f}_i(\mathbf{q}_i) = 0 \tag{19b}$$

$$\frac{\partial L_i}{\partial \boldsymbol{\lambda}_{g,i}} = 0, \text{ i.e. } \mathbf{G}_i(\mathbf{q}_i)\cdot\dot{\mathbf{q}}_i = 0 \tag{19c}$$

Introducing L_i from (18) in (19) and carrying out the required algebraic manipulation yields [11]:

$$\left[\frac{\partial V_i}{\partial \mathbf{q}_i} - \frac{d}{dt}\left(\frac{\partial V_i}{\partial \dot{\mathbf{q}}_i}\right)\right] - \boldsymbol{\lambda}_{e,i}^T\mathbf{J}_i + \boldsymbol{\lambda}_{g,i}\dot{\mathbf{q}}_i^T\left[\frac{\partial \mathbf{G}_i}{\partial \mathbf{q}_i} - \left(\frac{\partial \mathbf{G}_i}{\partial \mathbf{q}_i}\right)^T\right] - \dot{\boldsymbol{\lambda}}_{g,i}\mathbf{G}_i^T = 0 \tag{20}$$

which can be written in the form

$$\mathbf{h}_i^T(\mathbf{q}_i,\dot{\mathbf{q}}_i,\ddot{\mathbf{q}}_i,\boldsymbol{\lambda}_{g,i},\dot{\boldsymbol{\lambda}}_{g,i}) = \boldsymbol{\lambda}_{e,i}^T\mathbf{J}_i \tag{21a}$$

with

$$\mathbf{h}_i^T = \left[\frac{\partial V_i}{\partial \mathbf{q}_i} - \frac{d}{dt}\left(\frac{\partial V_i}{\partial \dot{\mathbf{q}}_i}\right)\right] + \boldsymbol{\lambda}_{g,i}\dot{\mathbf{q}}_i^T\mathbf{H}_i - \dot{\boldsymbol{\lambda}}_{g,i}\mathbf{G}_i^T \tag{21b}$$

$$\mathbf{H}_i = \left[\frac{\partial \mathbf{G}_i}{\partial \mathbf{q}_i} - \left(\frac{\partial \mathbf{G}_i}{\partial \mathbf{q}_i}\right)^T\right] \tag{21c}$$

Writing the Jacobian matrix $\mathbf{J}$ as $\mathbf{J} = \left[\mathbf{J}_m^T \,\vdots\, \mathbf{J}_{n-m}^T\right]$, where $\mathbf{J}_m^T = \left[\mathbf{J}^1\mathbf{J}^2\cdots\mathbf{J}^m\right]$, $\mathbf{J}_{n-m} = \left[\mathbf{J}^{m+1}\cdots\mathbf{J}^n\right]$ and $\mathbf{J}^i$ is the i-th column of $\mathbf{J}$, we define the matrix $\mathbf{Q} \in \Re^{n\times(n-m)}$:

$$\mathbf{Q} = \left[\mathbf{J}_{n-m}\quad \mathbf{J}_m^{-1} \,\vdots\, -\mathbf{I}_{n-m}\right]$$

where $\mathbf{I}_{n-m}$ is the *(n-m)* dimensional unit matrix, which consists of the null space basis vector of $\mathbf{J}$. One can easily verify that $\mathbf{J}\mathbf{Q}^T = \mathbf{0}$ and $\mathbf{J}^+\mathbf{Q}^T = 0$ where $\mathbf{J}^+ = \mathbf{J}^T(\mathbf{J}\mathbf{J}^T)^{-1}$ is the pseudoinverse of $\mathbf{J}$. This means that the column vectors of $\mathbf{J}^+$ together with column vectors of $\mathbf{Q}^T$ constitute the basis vectors of the *n-D* vector space. Thus any arbitrary *n-D* vector $\mathbf{a}$ can be expressed as $\mathbf{a} = \mathbf{J}^+\mathbf{b} + \mathbf{Q}^T\mathbf{c}$ where $\mathbf{b}$ and $\mathbf{c}$ are arbitrary *m-D* and *(n-m)-D* vectors, respectively. The vector $\dot{\mathbf{q}}_i$ is an *n-D* vector and so one has the expression:

$$\dot{\mathbf{q}}_i = \mathbf{J}_i^+\mathbf{b}_i + \mathbf{Q}_i^T\mathbf{c}_i \tag{22}$$

Introducing (22) into (4) yields the general solution of Eq (4) as:

$$\dot{\mathbf{q}}_i = \mathbf{J}_i^{+}\dot{\mathbf{x}}_{e,i}^{d} + \mathbf{Q}_i^{T}\mathbf{c}_i \tag{23}$$

where $\mathbf{Q}_i^{T}\mathbf{c}_i$ represents the homogeneous solution and $\mathbf{J}_i^{+}\mathbf{x}_{e,i}^{d}$ a particular solution. The vector $\mathbf{c}_i$ is called the *self-motion vector* (SMV). Now, transposing both sides of (21a) and premultiplying by $\mathbf{Q}_i(\mathbf{q}_i)$ yields:

$$\mathbf{Q}_i(\mathbf{q}_i)\mathbf{h}_i(\mathbf{q}_i,\dot{\mathbf{q}}_i,\ddot{\mathbf{q}}_i,\boldsymbol{\lambda}_{gi},\dot{\boldsymbol{\lambda}}_{gi}) = 0 \tag{24}$$

A good selection for the objective function V_i is:

$$V_i(\mathbf{q}_i,\dot{\mathbf{q}}_i) = \tfrac{1}{2}\dot{\mathbf{q}}_i^{T}\boldsymbol{\Sigma}_i\dot{\mathbf{q}}_i + \beta_i(\mathbf{q}_i) \tag{25}$$

where $\boldsymbol{\Sigma}_i$ is a suitable diagonal matrix and $\beta_i(\mathbf{q}_i)$ stands for the MM function used, e.g. the manipulability measure or the distance from an obstacle. Introducing (25) into (21b) yields:

$$\mathbf{h}_i(\mathbf{q}_i,\dot{\mathbf{q}}_i,\ddot{\mathbf{q}}_i,\boldsymbol{\lambda}_{g,i},\dot{\boldsymbol{\lambda}}_{g,i}) = (\nabla\beta_i) - \boldsymbol{\Sigma}_i\ddot{q}_i + \boldsymbol{\lambda}_{gi}\mathbf{H}_i^{T}\dot{\mathbf{q}}_i - \dot{\boldsymbol{\lambda}}_{gi}\mathbf{G}_i \tag{26}$$

Thus replacing the $\mathbf{h}_i$ from (26) in (24), where $\ddot{q}_i$ is computed by differentiating (23), here results:

$$\mathbf{Q}_i\left[(\nabla\beta_i) - \boldsymbol{\Sigma}_i\left(J_{eq,i}^{+}\dot{\mathbf{x}}_{e,i}^{d} + J_{eq,i}\ddot{\mathbf{x}}_{e,i}^{d} + \dot{\mathbf{Q}}_{eq,i}^{T}\mathbf{c}_i + \mathbf{Q}_{eq,i}^{T}\dot{\mathbf{c}}_i\right) + \boldsymbol{\lambda}_{gi}\mathbf{H}_i^{T}\dot{\mathbf{q}}_i - \dot{\boldsymbol{\lambda}}_{gi}\mathbf{G}_i\right] = 0$$

which can be written as:

$$\dot{\mathbf{c}}_{e,i} = \mathbf{C}_i^{-1}\mathbf{Q}\left[(\nabla\beta_i) - \boldsymbol{\Sigma}_i\left(\dot{\mathbf{J}}_{eq,i}^{+}\dot{\mathbf{x}}_{e,i}^{d} + \mathbf{J}_{eq,i}\ddot{\mathbf{x}}_{e,i}^{d} + \dot{\mathbf{Q}}_{eq,i}^{T}\mathbf{c}_i\right) + \boldsymbol{\lambda}_{gi}\mathbf{H}_i^{T}\dot{\mathbf{q}}_i\right] \tag{27}$$

where $\mathbf{c}_{e,i}^{T} = [c_i^{T} \;\vdots\; \boldsymbol{\lambda}_{gi}]$ and $\mathbf{C}_i = [\mathbf{Q}_i\boldsymbol{\Sigma}_i\mathbf{Q}_{eq,i}^{T} \;\vdots\; \mathbf{Q}_i\mathbf{G}_i]$.

Equations (23) and (27) form a set of $(2n-m)$ 1st-order nonlinear differential kinematic equations with n unknowns for $\mathbf{q}_i$ and $(n-m)$ unknowns for $\mathbf{c}_{e,i}$ which is an *equivalent self-motion vector* (ESMV).

For the first task, $\mathbf{q}_{1,0}$ (the initial configuration) is known but the initial value of the ESMV $\mathbf{c}_{e1,0}$ is unknown. Thus by setting $\mathbf{c}_{e1,0}$ we get $\mathbf{q}_1(t)$ and the final configuration $\mathbf{q}_{1,f}$. For the second task $\mathbf{q}_{2,0} = \mathbf{q}_{1,f}$ and by setting $\mathbf{c}_{e2,0}$ we get $\mathbf{q}_2(t)$ and $\mathbf{q}_{2,f}$. Proceeding this way we get the overall motion trajectory $\{\mathbf{q}_1(t),\mathbf{q}_2(t),\ldots,\mathbf{q}_N(t)\}$ and all the commutation configurations $\{\mathbf{q}_{1,f},\mathbf{q}_{2,f},\ldots,\mathbf{q}_{N,f}\}$. Since the SMV has not any influence on the end effector motion, one has to try to determine an optimal value of the SMV such that V_o in (16) is minimized. To this end one can use any numerical optimization technique (e.g. Powell's algorithm or tunelling algorithm)

4. Full-state Control of Mobile Manipulators

Several control laws and strategies have been proposed for mobile manipulators under different conditions and with various platform types. Since the MM's equations (9 a,b) or (12) are nonlinear, the feedback linearization is first applied to linearize the system equations. In robotics this method is known as the computed-torque control technique. Once the system is brought into linear form, any available linear control law can be applied with various levels of success.

The task of the end effector (end-point) of the MM is to track a desired trajectory $\mathbf{q}_d(t)$ in the world coordinate frame. Clearly, this cannot any time be achieved by the manipulator alone, without the help of the platform. In many cases the manipulator has to overstretch and almost reach the boundary of its workspace. Therefore what is usually done is to first control the mobile platform so as to bring the manipulator into a preferred configuration, e.g. the one with the maximum manipulability. The end effector position at/orientation to at the preferred configuration is then used as the reference point (set point) $\mathbf{q}_d$.

4.1 Feedback Linearizing Control

This technique has been applied by the authors to the full-state 2nd-order model of an omnidirectional MM:

$$\mathbf{A}(\mathbf{q})\ddot{\mathbf{q}} + \mathbf{B}(\mathbf{q})\dot{\mathbf{q}}\dot{\mathbf{q}} + \mathbf{C}(\mathbf{q})\dot{\mathbf{q}}^2 + \mathbf{F}\dot{\mathbf{q}} + \mathbf{G}(\mathbf{q}) = \tau \tag{28}$$

and to the state-space MM model (12).

The feedback linearizing control law for (28) is:

$$\tau = \mathbf{A}(\mathbf{q})\mathbf{u} + \mathbf{B}(\mathbf{q})\dot{\mathbf{q}}\dot{\mathbf{q}} + \mathbf{C}(\mathbf{q})\dot{\mathbf{q}}^2 + \mathbf{F}\dot{\mathbf{q}} + \mathbf{G}(\mathbf{q}) \tag{29}$$

and leads to:

$$\ddot{\mathbf{q}} = \mathbf{u} \tag{30}$$

where $\mathbf{u}$ is the "equivalent input" for the resulting system. The control law for $\mathbf{u}$ is then selected as:

$$\mathbf{u} = \ddot{\mathbf{q}}_d - 2\lambda\dot{\tilde{\mathbf{q}}} - \lambda^2\tilde{\mathbf{q}} \tag{31}$$

where $\mathbf{q}_d$ is the vector of the joint variable set points, λ is a strictly positive constant, and $\tilde{\mathbf{q}} = \mathbf{q} - \mathbf{q}_d$ is the position error.

Introducing (31) into (30) yields the error dynamic equation:

$$\ddot{\tilde{\mathbf{q}}} + 2\lambda\dot{\tilde{\mathbf{q}}} + \lambda^2\tilde{\mathbf{q}} = 0 \tag{32}$$

which (since $\lambda > 0$) converges exponentially to zero. The choice of the gain λ also ensures the exponential stability of the entire system.

4.2 Feedback Linearizing-Decoupling Control

Now, let us work with the state-space model (12). Let

$$\mathbf{y}(t) = \mathbf{c}(\mathbf{x}, t) + \mathbf{M}(\mathbf{x}, t)\tau \tag{33}$$

be the output equation, where $\mathbf{y}$ is the *m-D* MM's vector under control. The problem is to select $\mathbf{v}(\mathbf{x}, t)$ and $\mathbf{F}(\mathbf{x}, t)$ in the nonlinear feedback control law:

$$\tau(t) = \mathbf{v}(\mathbf{x}, t) + \mathbf{F}(\mathbf{x}, t)\mathbf{w}(t) \tag{34}$$

where $\mathbf{w}(t)$ is the new control vector of dimension m, such that the transfer function from $\mathbf{w}(t)$ to $\mathbf{y}(t)$ is linear and diagonal, i.e. each element $w_i(t)$ of $\mathbf{w}(t)$ controls only the corresponding element $y_i(t)$ of $\mathbf{y}(t)$. This is known as "*linearizing-decoupling control*".

To this end, we differentiate each element y_i as many times v_i as required until the coefficient of τ is nonzero. Namely:

$$\begin{aligned} y_i^{[j]} &= c_i^{[j]}(\mathbf{x},t) \\ y_i^{[v_i]} &= c_i^{[v_i]}(\mathbf{x},t) + \mu_i^{[v_i]}(\mathbf{x},t)\tau \end{aligned}, \quad i = 0,1,\ldots,v_i - 1 \tag{35}$$

where c_i, μ_i denote the i-th row of $\mathbf{c}(\mathbf{x},t)$ and $\mathbf{M}(\mathbf{x},t)$ respectively, and $y_i^{[j]}$ and $c_i^{[j]}$ denote the j-th time derivative of y_i and c_i, respectively. The integer v_i is equal to:

$$v_i = \min\left\{j:\ \mu_i^{[j]}(\mathbf{x},t) \neq 0,\ \ j = 0,1,2,\ldots\right\}$$

and is considered to be constant for all $(\mathbf{x},t)$ of interest.

Now, defining $\mathbf{c}^*(\mathbf{x},t)$, $\mathbf{M}^*(\mathbf{x},t)$, $\mathbf{\Lambda}$ and $\mathbf{a}^*(\mathbf{x},t)$

$$\mathbf{c}^*(\mathbf{x},t) = \begin{bmatrix} c_1^{[v_1]}(\mathbf{x},t) \\ \vdots \\ c_m^{[v_m]}(\mathbf{x},t) \end{bmatrix},\ \mathbf{M}^*(\mathbf{x},t) = \begin{bmatrix} \mu_1^{[v_1]}(\mathbf{x},t) \\ \vdots \\ \mu_m^{[v_m]}(\mathbf{x},t) \end{bmatrix},\ \mathbf{\Lambda} = \begin{bmatrix} \lambda_1 & & 0 \\ & \ddots & \\ 0 & & \lambda_m \end{bmatrix} \tag{36}$$

$$\mathbf{a}^*(\mathbf{x},t) = col\left[\sum_{k=0}^{v_i-1}\alpha_{ik}c_i^{[k]}(\mathbf{x},t)\right] = col\left[\sum_{k=0}^{v_i-1}\alpha_{ik}y_i^{[k]}\right]$$

where α_{ik} and λ_{ik}, $i = 1,2,\ldots,m$ are arbitrary constants, we find that the desired matrices of the control law (34) are given by:

$$\mathbf{v}(\mathbf{x},t) = -\mathbf{M}^*(\mathbf{x},t)\left[\mathbf{c}^*(\mathbf{x},t) + \mathbf{a}^*(\mathbf{x},t)\right] \tag{37a}$$

$$\mathbf{F}(\mathbf{x},t) = \mathbf{M}^{*-1}(\mathbf{x},t)\mathbf{\Lambda} \tag{37b}$$

Indeed, introducing in (12) and (33) the control law (34) with $\mathbf{v}$ and $\mathbf{F}$ given by (37a,b) yields:

$$y_i^{[v_i]} + \alpha_{i,v_i-1}y_i^{[v_i-1]} + \cdots + \alpha_{i,0}y_i = \lambda_i w_i,\ i = 1,2,\ldots,m \tag{38}$$

Now choosing suitable coefficients $\alpha_{i,k}$ and gains λ_i we can make each SISO system (38) possess desired poles (eigenvalues) or equivalently desired transient features.

4.3 Robust Sliding-mode Control

The above control laws assume that the MM's dynamic model is precisely known, which in practice is not always true, especially in the case of an MM. To overcome this fact, several robust controllers were proposed in the past for both linear and nonlinear systems [18]. In our case where the MM system is nonlinear s suitable robust control technique is the sliding mode control which can work even with severe parametric uncertainties. The authors have tested the sliding mode control on several types of robotic systems including industrial manipulators, biped robots and MMs [19, 20]. The sliding mode control technique is based on the so called "*sliding condition*":

$$\frac{1}{2}\frac{d}{ds}\mathbf{s}^T\mathbf{s} \leq -\eta(\mathbf{s}^T\mathbf{s})^{1/2},\ \eta > 0 \tag{39}$$

where $\mathbf{s} = \dot{\tilde{\mathbf{q}}} + \Lambda\tilde{\mathbf{q}}$ (see (28)) with Λ being a symmetric positive definite matrix. By formal manipulation one obtains:

$$\mathbf{s} = \dot{\tilde{\mathbf{q}}} + \Lambda\tilde{\mathbf{q}} = \dot{\mathbf{q}} - \dot{\mathbf{q}}_r, \ \dot{\mathbf{q}}_r = \dot{\mathbf{q}}_d - \Lambda\tilde{\mathbf{q}} \tag{40}$$

Now let us choose a Lyapunov function

$$V(t) = \frac{1}{2}\mathbf{s}^T\mathbf{A}\mathbf{s} \tag{41}$$

where $\mathbf{A}$ is the mass (inertia) matrix of the MM (see (28)). Through differentiating $V(t)$ and using (28) and (40) one obtains:

$$\dot{V}(t) = \mathbf{s}^T \ \tau - \mathbf{A}\ddot{\mathbf{q}}_r - \mathbf{C}\dot{\mathbf{q}}_r - \mathbf{F}\dot{\mathbf{q}}_r - \mathbf{G} \tag{42}$$

The control law is now selected as:

$$\tau = \hat{\tau} - \mathbf{k}\,\mathrm{sgn}(\mathbf{s}) \tag{43}$$

where the term $\mathbf{k}\,\mathrm{sgn}(\mathbf{s})$ is a vector with components $k_i\,\mathrm{sgn}(s_i)$. The control term $\hat{\tau}$ is selected such that to make $\dot{V}(t)$ be equal to zero if there is not a dynamic impression in the estimated dynamic model, i.e. as:

$$\hat{\tau} = \hat{\mathbf{A}}\ddot{\mathbf{q}}_r + \hat{\mathbf{C}}\dot{\mathbf{q}}_r + \hat{\mathbf{F}}\dot{\mathbf{q}}_r + \hat{\mathbf{G}} \tag{44}$$

where $\hat{\mathbf{A}}$, $\hat{\mathbf{C}}$, $\hat{\mathbf{F}}$ and $\hat{\mathbf{G}}$ are the estimated matrices of the MM. If $\mathbf{A}$, $\mathbf{C}$, $\mathbf{F}$ and $\mathbf{G}$ are the real matrices of the MM, the following errors are defined:

$$\tilde{\mathbf{A}} = \hat{\mathbf{A}} - \mathbf{A}, \ \tilde{\mathbf{C}} = \hat{\mathbf{C}} - \mathbf{C}, \ \tilde{\mathbf{G}} = \hat{\mathbf{G}} - \mathbf{G}, \ \tilde{\mathbf{F}} = \hat{\mathbf{F}} - \mathbf{F}$$

It is possible to select the components k_i of the vector $\mathbf{k}$ such that:

$$k_i \geq \left\| \left[\tilde{\mathbf{A}}(\mathbf{q})\ddot{\mathbf{q}}_r + \tilde{\mathbf{C}}(\mathbf{q},\dot{\mathbf{q}})\dot{\mathbf{q}}_r + \tilde{\mathbf{F}}\dot{\mathbf{q}}_r + \tilde{\mathbf{G}}(\mathbf{q}) \right] \right\| + \eta_i \tag{45}$$

with $\eta_i > 0$. It is not difficult to verify that using the control law {(43)-(44)} with the gains k_i satisfying the inequality condition (45), the following condition holds:

$$\dot{V}(t) \leq -\sum_{i=1}^{n} \eta_i |s_i| \leq 0 \tag{46}$$

which means that the sliding surface $\mathbf{s}$ is reached in a finite time and the MM's trajectories will remain on the surface. Thus they will converge to the desired (target) trajectory $\mathbf{q}_d(t)$ exponentially, despite the fact that the parameters $\hat{\mathbf{A}}$, $\hat{\mathbf{C}}$, $\hat{\mathbf{F}}$ and $\hat{\mathbf{G}}$ used in (44) are not the real (exact) ones.

5. Some Experimental Results

Our aim here is to give a set of representative results obtained by applying the motion planning and control techniques presented in Section 3 and Section 4.

5.1 MM Motion Planning Results

Consider an MM with a 2-DOF planar manipulator [11]:

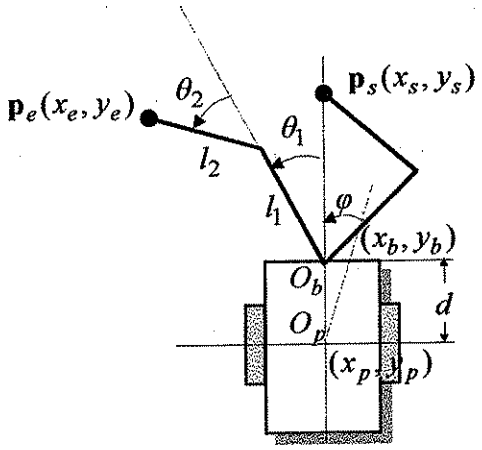

Figure 2. A Planar MM with 2-DOF Manipulator

If l_1 and l_2 are the link lengths and d is the distance from the platform center to the manipulator's base frame, then the MM kinematic equations are:

$$\begin{aligned} x_e &= x_p + d\cos\varphi + l_1\cos(\varphi+\theta_1) + l_2\cos(\varphi+\theta_1+\theta_2) \\ y_e &= y_p + d\sin\varphi + l_1\sin(\varphi+\theta_1) + l_2\sin(\varphi+\theta_1+\theta_2) \end{aligned} \tag{47}$$

with parameters values $l_1 = 0.5m$, $l_2 = 0.3m$ and $d = 0.25m$. The Jacobian matrix $\mathbf{J}$ is found to be:

$$\mathbf{J} = \begin{bmatrix} 1 & 0 & -d\cdot s\varphi - l_1\cdot s\varphi_1 - l_2\cdot s\varphi_{12} & -l_1\cdot s\varphi_1 - l_2\cdot s\varphi_{12} & -l_2\cdot s\varphi_{12} \\ 0 & 1 & -d\cdot c\varphi - l_1\cdot c\varphi_1 - l_2\cdot c\varphi_{12} & -l_1\cdot c\varphi_1 - l_2\cdot c\varphi_{12} & -l_2\cdot c\varphi_{12} \end{bmatrix} \tag{48}$$

where $s\varphi = \sin\varphi$, $s\varphi_1 = \sin(\varphi+\theta_1)$, $s\varphi_{12} = \sin(\varphi+\theta_1+\theta_2)$, $c\varphi = \cos\varphi$, $c\varphi_1 = \cos(\varphi+\theta_1)$, $c\varphi_{12} = \cos(\varphi+\theta_1+\theta_2)$. The extended Jacobian matrix $\mathbf{J}_e$ (see Eq. (6)) is found to be:

$$\mathbf{J}_e = \left[\begin{array}{ccccc} & & \mathbf{J} & & \\ \hline s\varphi & -c\varphi & 0 & 0 & 0 \end{array}\right] \tag{49}$$

Similarly $\mathbf{J}_m$ and $\mathbf{J}_{n-m}$ in $\mathbf{J} = \left[\mathbf{J}_m^T \;\vdots\; \mathbf{J}_{n-m}^T\right]$ are found to be:

$$\mathbf{J}_m = \begin{bmatrix} 1 & 0 \\ 0 & 1 \end{bmatrix},\ \mathbf{J}_{n-m} = \left[\begin{array}{c|c} -d\cdot s\varphi - l_1\cdot s\varphi_1 - l_2\cdot s\varphi_{12} & -d\cdot c\varphi - l_1\cdot c\varphi_1 - l_2\cdot c\varphi_{12} \\ -l_1\cdot s\varphi_1 - l_2\cdot s\varphi_{12} & -l_1\cdot c\varphi_1 - l_2\cdot c\varphi_{12} \\ -l_2\cdot s\varphi_{12} & -l_2\cdot c\varphi_{12} \end{array}\right] \tag{50}$$

and $\mathbf{J}_{e,m}$, $\mathbf{J}_{e,n-m}$ for $\mathbf{J}_e$ are found to be:

$$\mathbf{J}_{e,m} = \begin{bmatrix} 1 & 0 & s\varphi \\ 0 & 1 & -c\varphi \\ -d\cdot s\varphi - l_1\cdot s\varphi_1 - l_2\cdot s\varphi_{12} & -d\cdot c\varphi - l_1\cdot c\varphi_1 - l_2\cdot c\varphi_{12} & 0 \end{bmatrix} \tag{51}$$

$$\mathbf{J}_{e,n-m}=\begin{bmatrix} -l_1\cdot s\varphi_1-l_2\cdot s\varphi_{12} & -l_1\cdot c\varphi_1-l_2\cdot c\varphi_{12} & 0 \\ -l_2\cdot s\varphi_{12} & -l_2\cdot c\varphi_{12} & 0 \end{bmatrix} \tag{52}$$

The matrices $\mathbf{Q}$ and $\mathbf{Q}_e$ are found by using (50), (51) and (52) in the definition equations:

$$\mathbf{Q}=\left[\mathbf{J}_{n-m}\cdot\mathbf{J}_m^{-1}\ \vdots\ -\mathbf{I}_{n-m}\right],\ \mathbf{Q}_e=\left[\mathbf{J}_{e,n-m}\cdot\mathbf{J}_{e,m}^{-1}\ \vdots\ -\mathbf{I}_{n-m}\right]$$

A multitask was considered consisting of two sequential tasks defined by the equations:

$$\mathbf{x}_{e,1}=\begin{bmatrix}0.707t+0.889\\ 0.707t+0.389\end{bmatrix},\ \mathbf{x}_{e,2}=\begin{bmatrix}(t-3)+3.01\\ 2.51\end{bmatrix} \tag{53}$$

where a static force $\mathbf{f}=[0,10,0,0,0,0]^T N$ is exerted on the end effector in the 2nd task. The corresponding actuator torque vector is equal to:

$\tau_2=\mathbf{J}^T(\mathbf{q}_2)\mathbf{f}$

The objective function for the two tasks are:

$V_1(\mathbf{q}_1,\dot{\mathbf{q}}_1)=\frac{1}{2}\dot{\mathbf{q}}_1^T\dot{\mathbf{q}}_1$ (1st task)

$V_2(\mathbf{q}_2,\dot{\mathbf{q}}_2)=\frac{1}{2}\dot{\mathbf{q}}_2^T\dot{\mathbf{q}}_2+\frac{1}{2}\tau_2^T\tau_2$ (2nd task)

The platform considered is of the nonholonomic type with constraint

$G=\dot{x}_p\cos\varphi-\dot{y}_p\sin\varphi$

The resulting motion of this nonholonomic MM is shown in Figure 3, and the time variation of the torque norm $\frac{1}{2}\tau^T\tau$ in Figure 4.

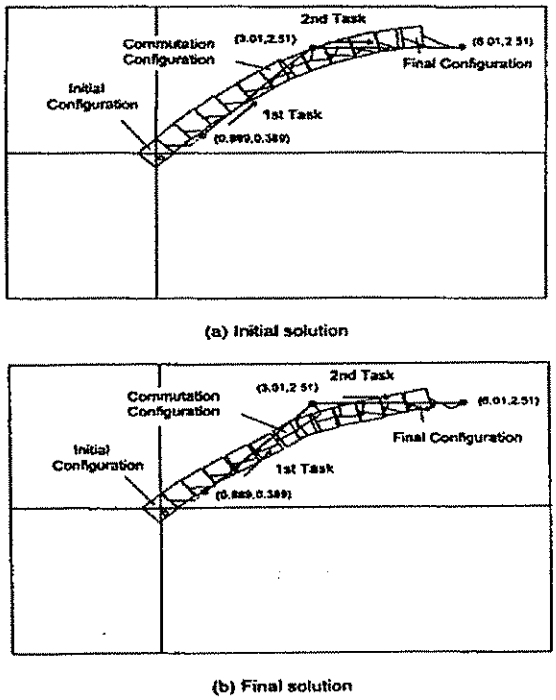

Figure 3. Initial and Final Solution for the Motion of the MM Performing A Double Task

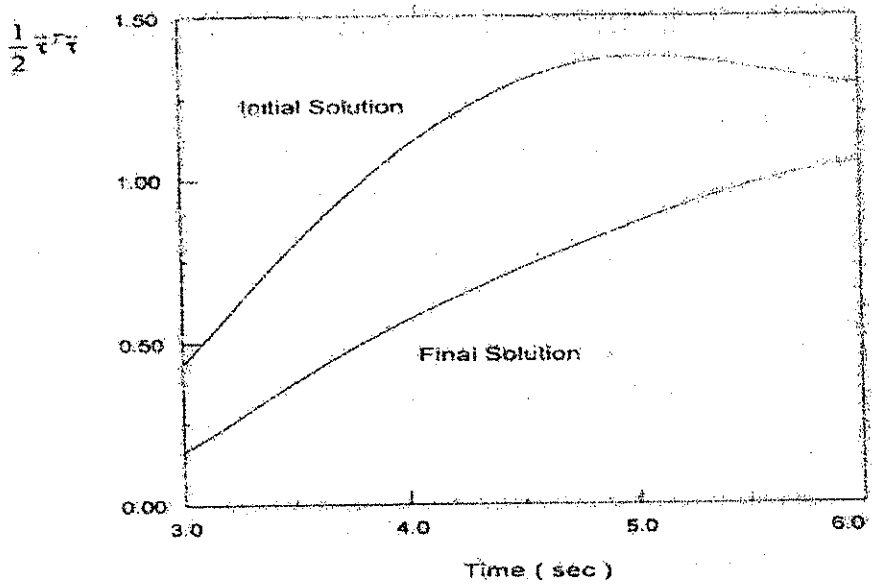

Figure 4. Torque Norm Variation for the MM Performing A Double Task

5.2 MM Sliding-Mode Control Results

The sliding-mode control has been applied to the omnidirectional MM shown in Figure 1b. The kinematic equations of this MM are:

$$\begin{aligned} {}^{w}x_e &= {}^{w}x_p + [l_2\cos\theta_2 + l_3\cos(\theta_2+\theta_3)]\cos(\varphi+\theta_1) \\ {}^{w}y_e &= {}^{w}y_p + [l_2\cos\theta_2 + l_3\cos(\theta_2+\theta_3)]\sin(\varphi+\theta_1) \\ {}^{w}z_e &= R_r + H + l_1 + l_2\sin\theta_2 + l_3\sin(\theta_2+\theta_3) \end{aligned} \tag{54}$$

where l_i $(i=1,2,3)$ are the link lengths, R_r is the radius of the wheels and H is the width of the platform. The Jacobian matrix $\mathbf{J}$ can be derived from (54) in the usual way. The MM's dynamic model has the form (28) where the matrices $\mathbf{A(q)}$, $\mathbf{B(q)}$, $\mathbf{C(q)}$ and $\mathbf{G(q)}$ have the standard meaning and $\mathbf{F}$ is a diagonal matrix containing the viscous coefficients.

The lengths of the links and the distance between the center of gravity of the platform and the wheel-assemblies are assumed to be exactly known. For all other parameters, we assume a bounded range of possible values for every parameter choosing the "mean" values of these ranges as the estimated parameters, and the "extreme" values of the ranges as the real parameters. The estimated values of the parameters used in the experiments are shown in Table 1.

Table 1. Numerical Values of the Mobile Manipulator's Parameters

Mass of each lateral orthogonal-wheel	0.5 K
Radius of the wheels	0.0245 m
Mass of the platform	30 Kg
Distance between the platform's center of gravity and each assembly	0.178 m
Moment of inertia of the platform with respect to z axis	0.93750 Kgm^2
Mass of link 1	1.25 m
Moment of inertia of link 1 with respect to x axis	0.01004 Kgm^2
Mass of link 2	4.17 Kg
Length of link 2	0.5 m
Position of the center of mass of link 2 along the link 2	0.25 m
Moment of inertia of link 2 with respect to x axis	0.34972 Kgm^2
Moment of inertia of link 2 with respect to z axis	0.00445 Kgm^2
Mass of link 3	0.83 Kg
Length of link 3	0.10 m
Position of the center of mass of link 3 along the link 3	0.05 m
Moment of inertia of link 3 with respect to x axis	0.00321 Kgm^2
Moment of inertia of link 3 with respect to z axis	0.00089 Kgm^2
Viscous coefficient for all rotational points	0.1 Nms

The real values of the parameters are given in Table 2.

Table 2. Real Numerical Values of the Mobile Manipulator Parameters

Mass of each lateral orthogonal-wheel	0.525 K (5% more)
Radius of the wheels	0.0245 m (exact)
Mass of the platform	33 K (10% more)
Distance between the platform's c. of g. and each assembly	0.178 m (exact)
Moment of inertia of the platform with respect to z axis	0.984375 Kgm^2 (5% more)
Mass of link 1	1.375 m (10% more)
Moment of inertia of link 1 with respect to x axis	0.010542 Kgm^2 (5% more)
Mass of link 2	5.421 Kg (30% more)
Length of link 2	0.5 m (exact)
Position of the center of mass of link 2 along the link 2	0.25 m (exact)
Moment of inertia of link 2 with respect to x axis	0.367206 Kgm^2 (5% more)
Moment of inertia of link 2 with respect to z axis	0.0046725 Kgm^2 (5% more)
Mass of link 3	1.0790 Kg (30% more)
Length of link 3	0.10 m (exact)
Position of the center of mass of link 3 along the link 3	0.05 m (exact)
Moment of inertia of link 3 with respect to x axis	0.0033705 Kgm^2 (5% more)
Moment of inertia of link 3 with respect to z axis	0.0009345 Kgm^2 (5% more)
Viscous coefficient (for all rotational joints)	0.13 Nms (30% more)

Two cases were considered: a straight-line trajectory and a circular trajectory of the platform's center of gravity. In both cases, a constant rotational velocity of 1° per second with respect to the absolute coordinate system is required for the platform. For the joint variables a ramp profile was chosen. The results for the circular trajectory are shown in Figure 5.

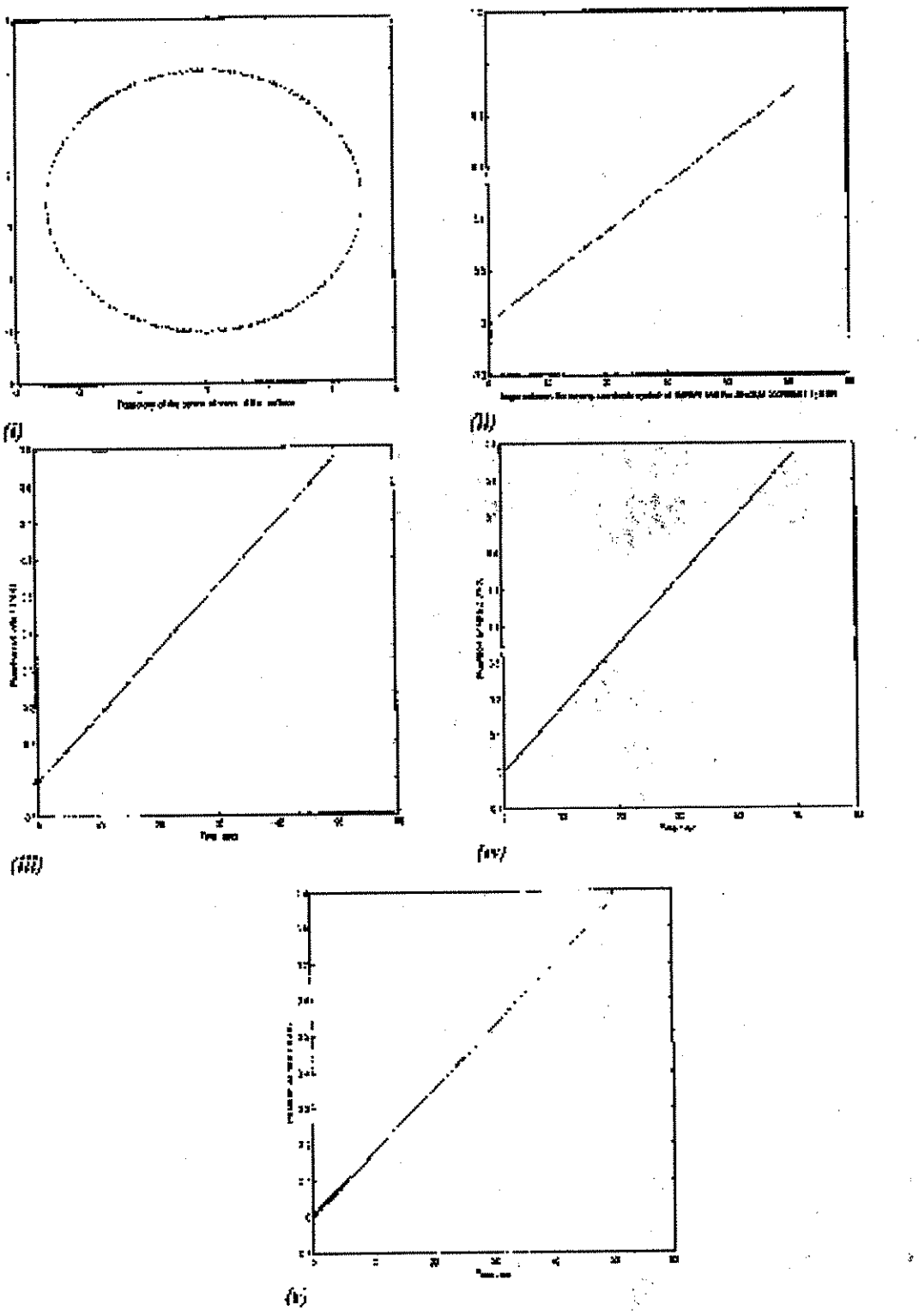

Figure 5. Robust Control of the MM: Circular Trajectory for the Platform's Center of Mass

The results for the straight-line trajectory are of similar quality, and show that the sliding controller is very robust with respect to large parameter's imprecision (uncertainty). Comparing these results with the ones obtained with the pure feedback linearizing computed torque controller, reveals the superiority of the sliding mode controller.

5.3 Two-step Feedback Linearizing-Decoupling Control

Consider the planar MM of Figure 2 which, in the frame $O_p - x_p y_p$, has the kinematic equations:

$$ {}^p\mathbf{p}_e = \begin{bmatrix} {}^p x_e \\ {}^p y_e \end{bmatrix} = \begin{bmatrix} {}^p x_b + l_1 \cos\theta_1 + l_2 \cos(\theta_1 + \theta_2) \\ {}^p y_b + l_1 \sin\theta_1 + l_2 \sin(\theta_1 + \theta_2) \end{bmatrix} \overset{\Delta}{=} \boldsymbol{\sigma}_2(\mathbf{q}_m) \tag{55} $$

In $O_p - x_p y_p$ the set point $\mathbf{p}_s(x_s, y_s)$ for the MM, i.e. for the arm's end point at the preferred configuration, is equal to:

$$ {}^p\mathbf{p}_s = \begin{bmatrix} {}^p x_s \\ {}^p y_s \end{bmatrix} = \begin{bmatrix} {}^p x_b + \left(l_1^2 + l_2^2\right)^{1/2} \\ {}^p y_b \end{bmatrix} \tag{56} $$

and obviously is a fixed position in O_p. The arm is in its preferred configuration if ${}^p\mathbf{p}_e = {}^p\mathbf{p}_s$. Therefore, the manipulator is driven into the preferred configuration if ${}^p\mathbf{p}_s$ is brought to ${}^w\mathbf{p}_e$ in the world coordinate frame O_w. From Figure 2 we find that:

$$ {}^w\mathbf{p}_s = \begin{bmatrix} {}^w x_s \\ {}^w y_s \end{bmatrix} = \begin{bmatrix} x_p + l_x \cos\phi - l_y \sin\phi \\ y_p + l_x \sin\phi + l_y \cos\phi \end{bmatrix} \overset{\Delta}{=} \boldsymbol{\sigma}_1(\mathbf{q}_p) \tag{57} $$

and

$$ {}^w\mathbf{p}_e = \begin{bmatrix} {}^w x_e \\ {}^w y_e \end{bmatrix} = \begin{bmatrix} x_p \\ y_p \end{bmatrix} + \begin{bmatrix} \cos\varphi & -\sin\varphi \\ \sin\varphi & \cos\varphi \end{bmatrix} {}^p\mathbf{p}_e \tag{58} $$

The set-point of ${}^p\mathbf{p}_e$ at time t is found by solving (58) with respect to ${}^p\mathbf{p}_e$. The output vector is selected to consist of the two components of ${}^p\mathbf{p}_e$ and the two components of ${}^w\mathbf{p}_s$, i.e.:

$$ \mathbf{y} = \begin{bmatrix} y_1 \\ y_2 \\ y_3 \\ y_4 \end{bmatrix} = \begin{bmatrix} {}^w x_s \\ {}^w y_s \\ {}^p x_e \\ {}^p y_e \end{bmatrix} = \begin{bmatrix} \boldsymbol{\sigma}_1(\mathbf{q}_p) \\ \boldsymbol{\sigma}_s(\mathbf{q}_m) \end{bmatrix} = \begin{bmatrix} \mathbf{c}_1(\mathbf{x}) \\ \mathbf{c}_2(\mathbf{x}) \end{bmatrix} \tag{59} $$

We observe that here the output equation (59) does not involve directly the input torque vector τ. Due to this and to the special structure of the MM's dynamic model (12) the following 2-step feedback linearizing-decoupling control procedure was proposed in [16, 17].

Step 1 Taking the equation for $\mathbf{x}_3$ in (12), i.e.

$$ \dot{\mathbf{x}}_3 = \mathbf{K}^{-1}\mathbf{C} + \mathbf{K}^{-1}\mathbf{S}\boldsymbol{\tau}, \quad \mathbf{x}_3 = \begin{bmatrix} \mathbf{v} \\ \dot{\mathbf{q}}_m \end{bmatrix} \tag{60} $$

we see that the control law

$$ \boldsymbol{\tau} = \mathbf{S}^{-1}(\mathbf{K}\mathbf{u} - \mathbf{C}) \tag{61} $$

gives $\dot{\mathbf{x}}_3 = \mathbf{u}$ which simplifies the model (12) as:

$$\dot{\mathbf{x}} = \mathbf{a}'(\mathbf{x}) + \mathbf{B}'(x)\mathbf{u}\,,\ \mathbf{a}'(x) = \begin{bmatrix} \mathbf{F}\mathbf{v} \\ \dot{\mathbf{q}}_m \\ 0 \end{bmatrix},\ \mathbf{B}'(x) = \begin{bmatrix} 0 \\ 0 \\ I \end{bmatrix} \tag{62}$$

Step 2 Through differentiating the sub-vectors $\mathbf{y}_{12} = [y_1, y_2]^T$ and $\mathbf{y}_{34} = [y_3, y_4]^T$ in (59) until $\mathbf{u}$ appears explicitly, and taking into account (62), we get:

$$\begin{aligned} \dot{\mathbf{y}}_{12} &= \dot{\mathbf{c}}_1(x) = \left(\frac{\partial \boldsymbol{\sigma}_1}{\partial \mathbf{q}_p}\right)\dot{\mathbf{q}}_p = \left(\frac{\partial \boldsymbol{\sigma}_1}{\partial \mathbf{q}_p}\mathbf{F}\right)\mathbf{v} \\ \ddot{\mathbf{y}}_{12} &= \ddot{\mathbf{c}}_1(x) = \left(\frac{\partial \boldsymbol{\sigma}_1}{\partial \mathbf{q}_p}\mathbf{F}\right)\dot{\mathbf{v}} + \left[\frac{d}{dt}\left(\frac{\partial \boldsymbol{\sigma}_1}{\partial \mathbf{q}_p}\mathbf{F}\right)\right]\mathbf{v} \end{aligned} \tag{63a}$$

$$\begin{aligned} \dot{\mathbf{y}}_{34} &= \dot{\mathbf{c}}_2(x) = \left(\frac{\partial \boldsymbol{\sigma}_2}{\partial \mathbf{q}_m}\right)\dot{\mathbf{q}}_m \\ \ddot{\mathbf{y}}_{34} &= \ddot{\mathbf{c}}_2(x) = \left(\frac{\partial \boldsymbol{\sigma}_2}{\partial \mathbf{q}_m}\right)\ddot{\mathbf{q}}_m + \left[\frac{d}{dt}\left(\frac{\partial \boldsymbol{\sigma}_2}{\partial \mathbf{q}_m}\right)\right]\dot{\mathbf{q}}_m \end{aligned} \tag{63b}$$

From (63a) and (63b) we obtain

$$\ddot{\mathbf{y}} = \mathbf{M}^*(\mathbf{x})\mathbf{u} + \dot{\mathbf{M}}^*(x)\mathbf{x}_3\,,\ \mathbf{M}^*(x) = \begin{bmatrix} \frac{\partial \boldsymbol{\sigma}_1}{\partial \mathbf{q}_p}\mathbf{F} & 0 \\ 0 & \frac{\partial \boldsymbol{\sigma}_2}{\partial \mathbf{q}_m} \end{bmatrix} \tag{64a}$$

To decouple the inputs and outputs of (64a) $\mathbf{u}$ must be selected such that:

$$\ddot{\mathbf{y}} = \boldsymbol{\Lambda}\mathbf{u} \tag{64b}$$

where the matrix $\boldsymbol{\Lambda}$ is diagonal and $\mathbf{w}$ is the new input vector.

From (64a) and (64b) we see that the desired input-output decoupling feedback control law is:

$$\mathbf{u} = \mathbf{M}^{*-1}(\mathbf{x})\left[\boldsymbol{\Lambda}\mathbf{u} - \dot{\mathbf{M}}^*(\mathbf{x})\mathbf{x}_3\right] \tag{65}$$

Of course $\mathbf{M}^*(\mathbf{x})$ should be nonsingular. This is so if the arm is not in any singular configuration and the set point $\mathbf{p}_s$ is not situated on the wheel axis.

A wide set of results has been produced for the following tasks:

- The arm's end effector must follow a straight -line.
- The arm's end effector has to follow a circular line.
- The platform has to follow a straight- line at a constant velocity along the y-direction in O_w and the arm is commanded independently, to follow an oscillatory motion along the x-axis relative to the vehicle frame.

In all cases, it has been verified that the full-state control gives much better tracking accuracy compared to the case where some or all of the interaction terms in Eq.(9a,b) are omitted. The resulting trajectory for the circular task is shown in Figure 6 [17].

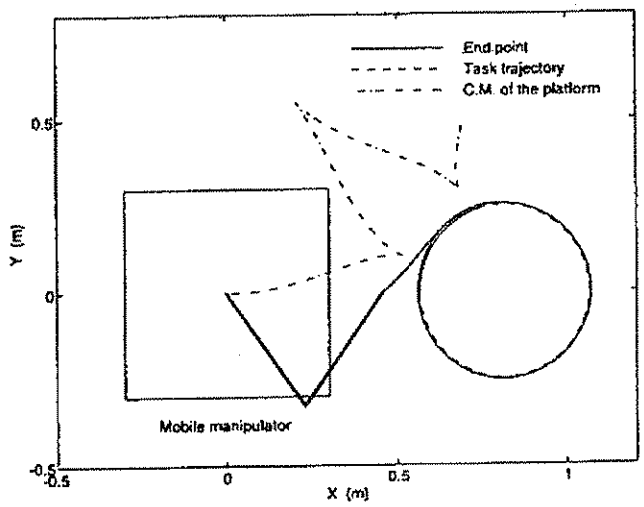

Figure 6. Simulation Trajectory for the Circular Path Task

6. Conclusions

The inclusion of the dynamic interaction terms (forces/torques) in the models and controllers of MMs ensures a much better tracking performance compared to the case where some or all of these terms are omitted. This has been verified in a number of simulation experiments by many authors including the authors of this paper. Over the years many types of control have been applied to mobile platforms, robotic manipulators and mobile manipulators. All of them use as a basis the feedback linearizing concept combined with other particular techniques. This paper focused on the sliding-mode control technique and on a special feedback linearizing and decoupling technique which is implemented in two steps. For the motion planning problem the Lee and Cho approach has been adopted, by which the commutation configurations and the motion trajectory are simultaneously obtained via numerical search. A minimal set of simulation results were included in the paper, to support the theoretical expectations. It remains to see how the above full-state controllers behave when applied to real MMs under real conditions. The authors are working towards applying full-state control on the ROBUTER MM which is available in Intelligent Robotics and Automation Laboratory.

REFERENCES

1. MUIR, P. F. and NEUMAN, C. P., **Kinematic Modeling of Wheeled Mobile Robots**, JOURNAL OF ROBOTIC SYSTEMS, Vol. 4, 1987, pp. 281-340.

2. GUY, C., GEORGES, B. and BRIGITTE, D., **Structural Properties and Classification of Kinematic and Dynamic Models of Wheeled Mobile Robots**, IEEE TRANSACTIONS ON ROBOTICS AND AUTOMATION, Vol. 12, No. 1, 1996, pp. 47-62.

3. PIN, F.G. and KILLOUGH, S. M., **A New Family of Omnidirectional and Holonomic Wheeled Platforms for Mobile Robots**, IEEE TRANSACTIONS ON ROBOTICS AND AUTOMATION, Vol. 10, No. 4, 1994, pp. 480-489.

4. WATANABE, K., SHIRAISHI, Y., TZAFESTAS, S. G., TAN, J. and FUKUDA, T., **Feedback Control of An Omnidirectional Autonomous Platform for Mobile Service Robots**, JOURNAL ON INTELLIGENT & ROBOTIC SYSTEMS, Vol. 22, Nos. 3-4, 1998, pp. 315-330.

5. WATANABE, K., SATO, K., IZUMI, K. and KUNITAKE, Y., **Analysis ad Control of An Omnidirectional Mobile Manipulator**, JOURNAL INTELLIGENT & ROBOTIC SYSTEMS, Vol. 27, Nos. 1-2, 2000, pp. 3-20.

6. TZAFESTAS, S. G., MELFI, A. and KRIKOCHORITIS, T., **Modeling and Control of An Omnidirectional Mobile Manipulator**, Proceedings of BASYS'2000: 4th IEEE/IFIP International Conference on Information Technology for Balanced Automation Systems, Berlin, Germany, September 27-29, 2000.

7. HAN, F., YAMADA, T., WATANABE, K., KIGUCHI, K. and IZUMI, K., **Construction of An Omnidirectional Mobile Robot Platform Based On Active Dual-wheel Caster Mechanisms and Development of A Control Simulator**, JOURNAL OF INTELLIGENT & ROBOTIC SYSTEMS, Vol. 29, 2000, pp. 257-275.

8. PIN, F. and CULIOLI, J.-C., **Optimal Positioning of Combined Mobile Platform-Manipulator Systems for Material Handling Tasks**, JOURNAL OF INTELLIGENT & ROBOTIC SYSTEMS, Vol. 6, 1992, pp. 165-182.

9. PIN, F., CULIOLI, J.-C. and REISTER, D. B., **Using Minimax Approaches to Plan Optimal Task Commutation Configurations for Combined Mobile Platform-Manipulator Systems**, IEEE TRANS.ACTIONS ON ROBOTICS AND AUTOMATION, Vol. 10, No. 1, 1994, pp. 44-45.

10. CARRIKER, W. F., KHOSLA, P. K. and KROGH, B.H., **Path Planning for Mobile Manipulators for Multiple Tasks Execution**, IEEE TRANSACTIONS ON ROBOTICS AND AUTOMATION, Vol. 7, No. 3, 1991, pp. 403-408.

11. LEE , J. K. and CHO, H.S., **Mobile Manipulator Motion Planning for Multiple Tasks Using Global Optimization Approach**, JOURNAL OF INTELLIGENT AND ROBOTIC SYSTEMS, Vol. 18, 1997, pp. 169-190.

12. JOSHI, J. and DESROCHERS, A. A., **Modeling and Control of A Mobile Robot Subject to Disturbances**, Proceedings of 1986 International Conference on Robotics and Automation, 1986.

13. DUBOWSKY, S. and TANNER, A. B., **A Study of Mobile Manipulators Subjected to Vehicle Disturbances**, Proceedings of the 4 th Symposium on Robot Research, 1987.

14. LIU, K. and LEWIS, F. L., **Decentralized Continuous Robust Controller for Mobile Robots**, Proceedings of the 1990 International Conference on Robotics and Automation, Cincinnati, Ohio, May 1990, pp. 1822-1827.

15. HOOTSMANNS, N. A. M. and DUBOWSKI, S., **The Motion Control of Manipulators on Mobile Vehicles**, Proceedings of IEEE International Conference on Robotics and Automation (ICRA'91), 1991, pp. 2336-2341.

16. YAMAMOTO, Y. and YUN, X., **Coordinating Locomotion and Manipulation of A Mobile Manipulator**, IEEE TRANSACTIONS ON AUTOMATIC CONTROL, Vol. 39, 1994, pp. 1326-1332.

17. YAMAMOTO, Y. and YUN, X., **Effect of the Dynamic Interaction on Coordinated Control of Mobile Manipulators**, Vol. 12, 1996, pp. 816-824.

18. SLOTINE, J. and LI, W., **Applied Nonlinear Control**, PRENTICE HALL, 1991.

19. TZAFESTAS, S. G., RAIBERT, M. and TZAFESTAS, C. S., **Robust Sliding Mode Control Applied to A 5-Link Biped Robot,** JOURNAL OF INTELLIGENT AND ROBOTIC SYSTEMS, Vol. 15, No. 1, 1996, pp. 67-133.

20. TZAFESTAS, S. G., KRIKOCHORITIS, T.E. and TZAFESTAS, C. S., **Robust Sliding Mode Control of A 9-Link Biped Robot Walking**, JOURNAL OF INTELLIGENT AND ROBOTIC SYSTEMS, Vol. 20, Nos. 2-4, 1997, pp. 375-402.

21. MEGHDARI, A., DURALI, M. and NADERI, D., **Investigating Dynamic Interaction Between the One DOF Manipulator and Vehicle of A Mobile Manipulator**, JOURNAL OF INTELLIGENT AND ROBOTIC SYSTEMS, Vol. 28, 2000, pp. 277-290.